Synchronization and Desynchronization in a Network of Locally Coupled Wilson–Cowan Oscillators

Shannon Campbell and DeLiang Wang, *Member, IEEE*

***Abstract*— A network of Wilson–Cowan (WC) oscillators is constructed, and its emergent properties of synchronization and desynchronization are investigated by both computer simulation and formal analysis. The network is a two-dimensional matrix, where each oscillator is coupled only to its neighbors. We show analytically that a chain of locally coupled oscillators (the piecewise linear approximation to the WC oscillator) synchronizes, and present a technique to rapidly entrain finite numbers of oscillators. The coupling strengths change on a fast time scale based on a Hebbian rule. A global separator is introduced which receives input from and sends feedback to each oscillator in the matrix. The global separator is used to desynchronize different oscillator groups. Unlike many other models, the properties of this network emerge from local connections, that preserve spatial relationships among components, and are critical for encoding Gestalt principles of feature grouping. The ability to synchronize and desynchronize oscillator groups within this network offers a promising approach for pattern segmentation and figure/ground segregation based on oscillatory correlation.**

I. Introduction

THE ability to extract salient sensory features from a perceived scene or sensory field, and group them into coherent clusters, or objects, is a fundamental task of perception. These abilities are essential for figure/ground segregation, object segmentation, and pattern recognition. There are two forms of sensory segmentation: peripheral segmentation, which is based on the correlation of local qualities within a pattern, and central segmentation, which is based on prior knowledge about patterns. As the techniques for single object recognition become more advanced, the need for efficient segmentation of multiple objects grows, since both natural scenes and manufacturing applications of computer vision are rarely composed of a single object [34], [52].

Though it is known that different features, e.g., orientation, color and direction of motion, are processed in different cortical areas [71], it is unknown how those features are integrated, or grouped, into the perception of a coherent object. When there are multiple objects with many features, the number of possible linkages between them grows combinatorially. How these features are correctly bound together to form objects is known as the feature binding problem. Theoretical considerations of brain functions suggest temporal correlations of neural activity as a representational framework for perceptual grouping [44], [62], [2]. In the correlation theory of von der Malsburg and Schneider [64], features are linked through temporal correlations in the firing patterns of different neurons. A natural implementation of temporal correlation is the use of neural oscillators, whereby each oscillator represents some feature (maybe just a picture element, or a pixel) of an object. In this scheme, each segment (object) is represented by a group of oscillators that are synchronized (phase-locked). Different objects are represented by different groups whose oscillations are desynchronized from each other. Following Wang and Terman [69], [60], we refer to this form of temporal correlation as oscillatory correlation. Given that brain waves are widespread in EEG recordings [38], and the ubiquitous nature of the 40 Hz oscillations, it is possible for the brain to use oscillatory correlation as a method of solving the binding problem.

Recently, the theory of oscillatory correlation has received direct support from neural recordings in the cat visual cortex [17], [31] and other brain regions. We summarize the findings relevant to this work as follows:

1) Neural oscillations are triggered by sensory stimulation, i.e., they are stimulus driven.
2) Global phase locking of neural oscillations with zero phase shift occurs when the stimulus is a coherent object, e.g., a long visual bar, or strongly correlated, e.g., the same location.
3) No phase locking occurs across different stimuli if they are not related to one another, e.g., they do not have the same direction or orientation.

These basic findings have been confirmed by later experiments which demonstrate that phase locking can occur between the striate cortex and the extrastriate cortex [19], and between the two striate cortices of the two hemispheres [20]. Also, phase-locking has been observed across the sensorimotor cortex in awake monkeys [47], [51].

The experimental findings in the cat visual cortex have created much interest in the theoretical community. Models simulating the experimental results have been proposed [55], [40], [32], [57], [13], [28], [65], [66], as well as models exploring the ability of oscillatory correlation to solve the problems of pattern segmentation and figure/ground segregation [58], [6], [63], [46]. While some of these models demonstrate synchronization with local couplings [40], [56], [65], [69], 60], most rely on long-range connections to achieve entrainment, since global connectivity can readily result in synchrony (see [29] for specific conditions). It has been argued that local con-

Manuscript received May 29, 1994; revised November 10, 1994. This work was supported in part by ONR Grant N00014-93-1-0335 and NSF Grant IRI-9211419.

S. Campbell is with the Department of Physics, Ohio State University, Columbus, OH 43210-1277 USA.

D. Wang is with the Laboratory for Artificial Intelligence Research, Department of Computer and Information Science and Center for Cognitive Science, Ohio State University, Columbus, OH 43210-1277 USA.

Publisher Item Identifier S 1045-9227(96)01227-1.

nections may play a fundamental role in pattern segmentation, because global couplings lack topological mappings [58], [66]. Specifically, in a two-dimensional (2-D) array of oscillators, where each oscillator represents an element in a sensory field, all to all couplings indiscriminately connect multiple objects. All pertinent geometrical information about each object, and about the spatial relationships between objects is lost. Because this spatial information is necessary for object recognition and segmentation, it must be preserved as effectively and as simply as possible. The use of local couplings is one method of maintaining such spatial relationships.

In this paper, we study a network of locally coupled Wilson–Cowan (WC) oscillators [70]. In particular, we investigate the properties of synchronization and desynchronization in such networks. Each oscillator is a two-variable system of ordinary differential equations, and represents an interacting population of excitatory and inhibitory neurons. The amplitudes of the variables symbolize the proportion of each population of neurons that is active. We use these equations because they represent neuronal groups, which may be the basic processing units in the brain [18]. In our model, each oscillator is analogous to a basic element in a sensory field, and responds only to the presence of stimulus. The WC equations have a large number of parameters, which allow for a wide range of dynamics. These equations have been used widely in modelling various brain processes [24], [5], [40], [10], in creating oscillatory recall networks [68], and in exploring the binding problem [35], [63], [66]. Because of the neurophysiological importance of the WC equations, several authors have examined their mathematical properties [22], [39], [5], [23], [12]. Of particular relevance is a study by Cairns *et al.* [12], which indicates that synchronization is possible with these equations. Despite extensive studies on WC oscillators, it remains unclear to what extent a locally coupled network can exhibit global synchrony, and whether desynchronization can be achieved in different regions of the network, useful in many contexts.

The two main aspects of the theory of oscillatory correlation are synchronization within an object, and desynchronization between objects. In many models synchronization is achieved, but the issue of desynchronization is not addressed. Objects in these models oscillate independently of one another. This independence allows for the possibility of accidental synchrony [36]. Accidental synchrony occurs when two or more objects are incorrectly grouped together because they have the same, or indistinguishable, phases. The probability that two objects are wrongly grouped can be substantial, however, when one considers that synchrony is rarely perfect. The effects of noise and the length of time needed to achieve synchrony require that a tolerance of phase differences be allowed. In addition, note that as the number of objects increases, the probability of erroneously correlating different objects increases significantly. Several authors [58], [40], [66] avoid the problem of accidental synchrony by averaging over a number of trials. Though this greatly reduces the chance of accidentally aligning the phases of two different objects, it does so at the cost of substantially increasing the computational time.

There are few models that incorporate a method of desynchronization. Terman and Wang [60] give a rigorous analysis of desynchronization in coupled relaxation oscillators. Relaxation oscillators, however, have two time scales and are based on models of single cell voltages, so the analysis of Terman and Wang may not be applicable to the widely used WC oscillators. In the simulations of von der Malsburg and Buhmann [63], an approximation to the WC equations is used, and a global inhibitor desynchronizes two segments, each corresponding to a group of fully connected oscillators. But their simulations involve a small system and no analysis is made. It is also unknown how their results extend to more than two objects. In the model of Schillen and König [53], the phases of two different objects are anti-correlated by desynchronizing connections between the objects. These desynchronizing connections are short range, however, and two objects can oscillate independently if separated by a large enough distance.

In our model desynchronization of multiple objects is accomplished with a global separator (GS), which receives input from the entire network, and feeds back to all oscillators. These global connections to and from GS make this architecture resemble that of the comparator model [37]. The comparator model uses long-range connections to and from a comparator, a unit which commonly computes the average phase of all oscillators, to achieve synchrony. This architecture, however, phase locks every oscillator. Desynchronization then becomes problematic. In direct contrast, our model uses long-range couplings with GS to decisively separate objects, thus eliminating the need to average over repeated trials. Long-range connections serve to adjust the relative phases between oscillator groups, wherever they may be on the network. The model we present uses short range coupling to achieve synchrony, while global couplings with GS give rise to desynchronization. This simple architecture may provide an efficient approach to pattern segmentation and a computational foundation for feature binding.

The model is described in the following section. In Section III, it is proven that synchrony is the globally stable solution for a chain of oscillators given sufficient coupling strength, and a technique for fast entrainment is presented. GS and the dynamics of desynchronization are described in Section IV. Computer simulations of a 2-D network with five objects are shown in Section V. In Section VI we discuss possible extensions to our model.

II. Model Definition

The basic architecture of the model is shown in Fig. 1. GS is connected to the entire network. The connections between oscillators are local. An oscillator located on a black square can only be coupled with oscillators on adjacent diagonally striped squares. The topology of the network is a rectangle, not a torus. The coupling strengths are dynamically changed on a fast time scale compared to the period of the oscillations (further discussion below). The dynamic couplings serve to increase the coupling strength between units that are active, to decrease the coupling strength between excited units and

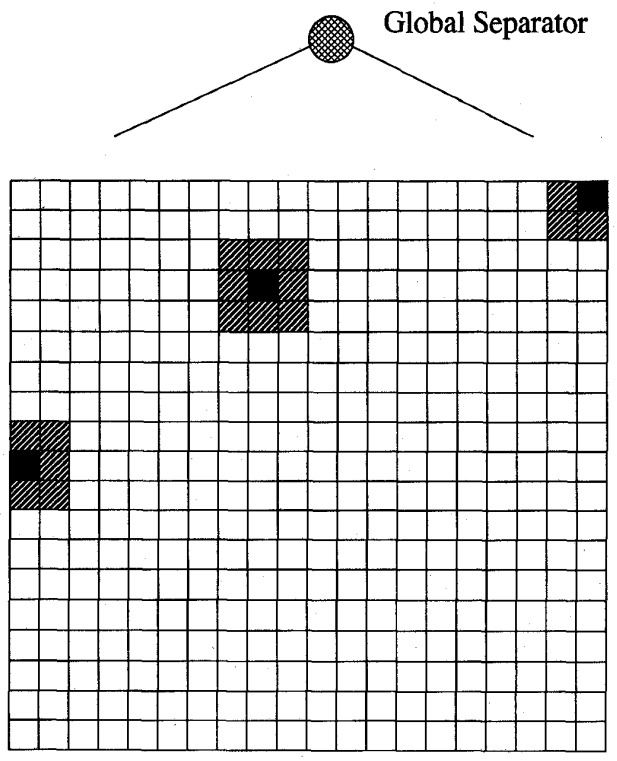

Fig. 1. Basic architecture of the model. The oscillators are arranged in a 2-D grid, where each square on the grid represents an oscillator. The connections between oscillators are local. Three representative situations are shown in the figure, where an oscillator located at a black site is connected only to oscillators on adjacent striped squares. Note that we do not use periodic boundary conditions. The Global Separator (GS) is pictured at the top and is coupled with all oscillators in the network.

inactive units, and to decrease the connection strength between two silent units, all rapidly and temporarily.

Each functional element on the grid is a simplified WC oscillator defined as

$$\dot{x}_i = -x_i + H(ax_i - by_i - \phi_x + \sigma_z + I_i + \rho) + \alpha S_{xi} \tag{1a}$$

$$\dot{y}_i = \eta(-y_i + H(cx_i + dy_i - \phi_y)) + \alpha S_{yi} \tag{1b}$$

$$H(v) = (1 + \exp(-v))^{-1}. \tag{1c}$$

The parameters have the following meanings: a and d are the values of self excitation in the x and units, respectively. b is the strength of the coupling from the inhibitory unit, y, to the excitatory unit, x. The corresponding coupling strength from x to y is given by c. ϕ_x and ϕ_y are the thresholds. Fig. 2 shows the connections for single oscillator. The x and y variables are interpreted as the proportion of active excitatory and inhibitory neurons, respectively. η modifies the rate of change of the y unit. ρ is a noise term. The noise is assumed to be Gaussian with statistical property

$$\langle \rho(t) \rangle = 0 \tag{2a}$$

$$\langle \rho(t)\rho(t') \rangle = 2D\delta(t - t') \tag{2b}$$

where D is the amplitude of the noise and $\delta(t-t')$ is the Dirac delta function. The ith oscillator receives a binary input I_i. A

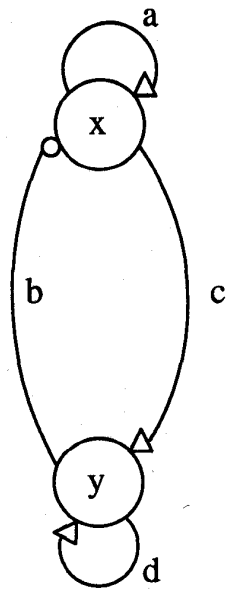

Fig. 2. A diagram showing the connections that each excitatory and inhibitory unit has within an oscillator. Triangles represent excitatory connections, and circles represent inhibitory connections.

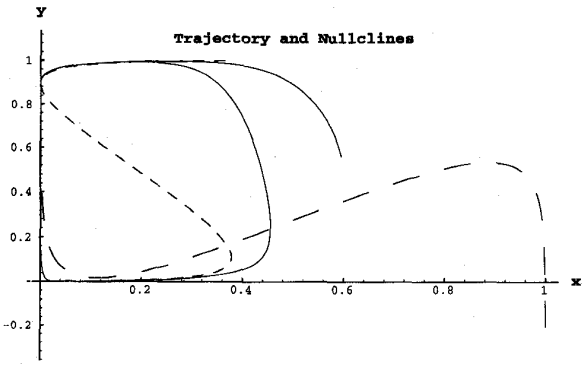

Fig. 3. The y nullcline (small dashes), x nullcline (large dashes), and trajectory (solid) for a single oscillator are displayed. The parameters are $a = 10.0, b = 7.0, \phi_x = 4.075, c = 10.0, d = 10.2129, \phi_y = 7.0, \sigma = 2.1$, $\rho = 7.0$, and $D = 0$.

value of $I_i = 1$ corresponds to those parts of the sensory field that are stimulated and drives the oscillator into a periodic regime. Oscillators that do not receive input, namely $I_i = 0$, remain silent. z represents the activity of GS and will be specified in detail in Section IV. Though it may seem unusual to denote the position of an oscillator in a 2-D array with only one index, we do so to avoid using four indexes to label the connections between oscillators. Fig. 3 displays the nullclines, the curves along which the values of $\dot{x}$ or $\dot{y}$ are zero, and the trajectory of a point near the limit cycle. The caption of Fig. 3 lists values for the parameters $a, b, c, \sigma, \rho, d, \phi_x, \phi_y$ and D.

The interaction terms are given by

$$S_{xi} = -\kappa_i x_i + \sum_j J_{ij} x_j \tag{3a}$$

$$S_{yi} = -\kappa_i y_i + \sum_j J_{ij} y_j \tag{3b}$$

where the sum is over $j \in N(i)$, and $N(i)$ is the set of neighbors that element i has. We call this form of coupling scalar diffusive coupling. This terminology originates from Aronson *et al.* [4], who use the term "scalar coupling" to denote interactions in which the coupling strength is identical for both the x and y variables. We add in "diffusive" to specify the form of coupling. The interaction term was initially included in the sigmoid terms of (1) when we began experimenting with this network. When the sigmoidal function is expanded in a Taylor series in terms of the coupling strength, however, it can be shown that the first-order term is proportional to the linear coupling specified in (1). Thus, to simplify the mathematical analysis we perform later in this paper, the interaction terms are not presently included in the nonlinearities. The terms $\kappa_i(t)$ and $J_{ij}(t)$ are specified below.

The connections between the oscillators are allowed to change on a fast time scale, as first suggested by von der Malsburg [62], [64]. They obey the following Hebbian rule: the connections between excited oscillators increase to a maximum, the connections between excited and unstimulated oscillators decrease to zero, and the connections between unstimulated oscillators decrease to zero. This rule uses of a pair of connection weights. The permanent links $T_{ij}^1 s$ denote existence of connections between i and j, and reflect the architecture of the network (locally connected 2-D grid, see Fig. 1). The dynamic links J_{ij}'s change on a fast time scale compared to the period of oscillation, and represent the efficacy of the permanent links. The idea of fast synaptic modulation is introduced on the basis of its computational advantages and neurobiological plausibility [62], [64]. The permanent links are given by $T_{ij} = 1$ if i, j are neighbors and $T_{ij} = 0$ otherwise. The dynamic links are computed as follows:

$$J_{ij} = T_{ij} h(\langle x_i \rangle) h(\langle x_j \rangle) \tag{4}$$

where $h(\langle x_i \rangle)$ is a measure of the activity of oscillator i. It is defined as $h(\langle x_i \rangle) = \Theta(\langle x_i \rangle - \varphi)$, where φ is some threshold, and Θ is the Heaviside step function. Namely $h(\langle x_i \rangle) = 1$ if the temporal average of activity, $\langle x_i \rangle$, is greater than the threshold, or $h(\langle x_i \rangle) = 0$ if otherwise. With (4) in place, only neighboring excited oscillators will be effectively coupled. This is an implicit encoding of the Gestalt principle of connectedness [50].

With scalar diffusive coupling, the Hebbian rule defined above would destabilize the synchronous solution. To understand how the instability arises, consider three excited oscillators arranged in a row, and each with the same values of activities, i.e., $x_1 = x_2 = x_3$, and $y_1 = y_2 = y_3$. Because of the Hebbian coupling rule, the middle oscillator has the following interaction term $-\kappa_2 x_2 + x_1 + x_3 = (2 - \kappa_2) x_1$, while the first and third oscillators have the interaction terms $-\kappa_1 x_1 + x_2 = (1 - \kappa_1) x_1$ and $-\kappa_3 x_3 + x_2 = (1 - \kappa_3) x_1$ respectively. These interaction terms are different, and cause the trajectories of the oscillators to be different. An exact synchrony is not possible. An obvious solution is to change $\kappa_i(t)$ so that it equals the number of excited neighbors that oscillator i is coupled with. We set

$$\kappa_i(t) = \sum_j J_{ij}(t) \tag{5}$$

so that the interaction terms will be zero when the oscillators are synchronized. All the oscillators will now have the same trajectory and remain synchronous. The effect of (5) is similar to the dynamic normalization introduced by Wang [65], [66]. The original form of dynamic normalization served to normalize the connection strengths between oscillators. In this model we do not normalize connection strengths, but instead alter the multiplicative constant on the scalar diffusive coupling term. Either formulation would have the same results with these equations, but we choose to normalize the multiplicative constant because it is more direct. The effect of dynamic normalization is to maintain a balanced interaction term so that coupled oscillators remain synchronous independent of the number of connections that they have.

The architecture of this network allows us to implement the basic aspects of oscillatory correlation, synchrony and desynchrony. To illustrate, assume that the network receives input as shown in Fig. 4. The black squares represent units that receive stimulation, and these units then produce oscillatory behavior. The dynamic couplings will disconnect excited units from unexcited units, and group connected units together. For the five objects pictured in the input, there will be five corresponding groups of oscillators. Connected oscillators synchronize, and GS ensures that no two spatially separated objects have the same phase.

III. Synchronization

Much work has been done with coupled phase oscillators [41], [16], [59], [21], [23], [57] because the phase model is the simplest description of a smooth limit cycle. Phase oscillators are generally defined as

$$\dot{\phi}_i = \omega_i + \sum_j K_{ij} G(\phi_i - \phi_j) \tag{6}$$

where ϕ_i is the phase of the ith oscillator, ω_i is its intrinsic frequency. K_{ij} is the coupling strength between the ith and the jth oscillators, G and is a 2π periodic function. For phase oscillators with local diffusive coupling, and identical intrinsic frequencies, the in-phase solution is asymptotically stable [14]. But the phase model does not exhibit the rich variety of behaviors that other, more complex nonlinear oscillators, have when locally coupled. For the so called Brusselator, a model of chemical oscillation, stable states can arise or disappear, depending on initial conditions and the coupling strength [7]. Moreover, if the ratio of the coupling strengths is explored, period doubling bifurcations and chaos can develop [54]. Neu [48] gives a general result describing synchrony for locally coupled oscillators, but it is obtained by taking a continuum limit, and requiring that some of the oscillators be initially synchronized. Because the system of WC oscillators that we use differs significantly from those mentioned above, we examine the properties of the following approximation to the WC oscillator in detail. We show that with a sufficiently

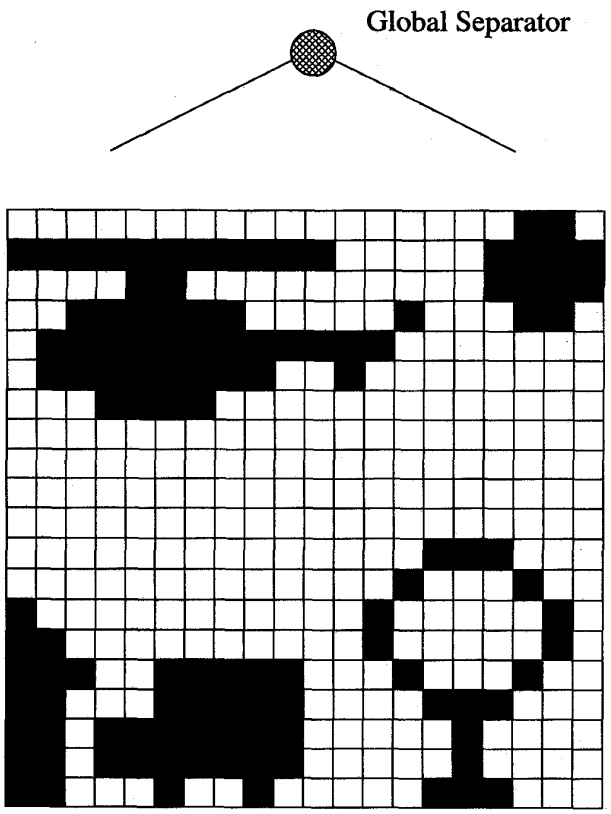

Fig. 4. Input used for the network. Black squares denote oscillators that receive input. Starting clockwise from the upper left-hand corner, we name the objects as follows: a helicopter, a thick addition sign, a tree, a truck, and a house.

large coupling strength synchrony occurs for a finite number of oscillators, independent of their initial conditions.

Using basic matrix stability analysis, we show that a chain of oscillators can achieve synchrony. The equations we analyze are a bit different from those shown in (1). We do not include parameter $\eta, D = 0$, and we do not consider the effects of GS. We have also dropped the S notation because the interaction terms can be explicitly included. A diagram of the connections between units, arranged in a chain, is given in Fig. 5. Note that the two ends are not connected with one another. Thus we are analyzing a chain, not a ring, of n oscillators. The equations are

$$\dot{x}_1 = -x_1 + P(ax_1 - by_1 - \varphi_x) + \alpha(x_2 - x_1) \tag{7a}$$

$$\dot{y}_1 = -y_1 + P(cx_1 + dy_1 - \varphi_y) + \alpha(y_2 - y_1) \tag{7b}$$

$$\vdots$$

$$\dot{x}_i = -x_i + P(ax_i - by_i - \varphi_x) + \alpha(x_{i+1} + x_{i-1} - 2x_i) \tag{7c}$$

$$\dot{y}_i = -y_i + P(cx_i + dy_i - \varphi_y) + \alpha(y_{i+1} + y_{i-1} - 2y_i) \tag{7d}$$

$$\vdots$$

$$\dot{x}_n = -x_n + P(ax_n - by_n - \varphi_x) + \alpha(x_{n-1} - x_n) \tag{7e}$$

$$\dot{y}_n = -y_n + P(cx_n + dy_n - \varphi_y) + \alpha(y_{n-1} - y_n) \tag{7f}$$

where the sigmoid function $H(v)$ has been approximated with

$$P(v) = \begin{cases} 0 & \text{if } v < -e \\ v/(2e) + 1/2 & \text{if } -e \le v \le e \\ 1 & \text{if } v > e. \end{cases} \tag{8}$$

The constants a, b, c, d, φ_x, and φ_y are positive values, $\log(e) = 1$, and α is the coupling strength. We now state our major analytical result as the following theorem.

Theorem: For the system of coupled oscillators defined in (7) and (8), the coupling strength α can be chosen such that synchrony is asymptotically stable.

Proof: First, let $a^2 + b^2 > c^2 + d^2$, and let us define the following notations:

$$\begin{aligned} \bar{r}_i &= (x_i - x_{i+1}, y_i - y_{i+1}), \\ r_i^2 &= (x_i - x_{i+1})^2 + (y_i - y_{i+1})^2 \end{aligned} \tag{9}$$

$$\cos(\theta_i) = \frac{(x_i - x_{i+1})}{r_i}, \quad \text{and} \quad \sin(\theta_i) = \frac{(y_i - y_{i+1})}{r_i} \tag{10}$$

$$f_i = P(ax_i - by_i - \varphi_x) - P(ax_{i+1} - by_{i+1} - \varphi_x) \tag{11a}$$

$$g_i = P(cx_i + dy_i - \varphi_y) - P(cx_{i+1} + dy_{i+1} - \varphi_y). \tag{11b}$$

Note that $\bar{r}_i$ is a two element vector, and r_i is the positive square root of r_i^2. The time derivative of the distance between two oscillators can be written as

$$\frac{1}{2}\frac{d}{dt}r_i^2 = \bar{r}_i \cdot \dot{\bar{r}}_i = r_i \dot{r}_i. \tag{12}$$

We will use the "dot" above a variable to denote its first order time derivative. According to (7) we can write

$$\begin{aligned} r_i \dot{r}_i = &-(1 + 2\alpha)r_i^2 + (r_i \cos(\theta_i) f_i + r_i \sin(\theta_i) g_i) \\ &+ \alpha(\bar{r}_i \cdot \bar{r}_{i-1} + \bar{r}_i \cdot \bar{r}_{i+1}). \end{aligned} \tag{13}$$

In the above equation $1 \le i \le n - 1$, and let the values of the undefined variables $r_0 = r_n = 0$. The functions f_i and g_i are bounded by

$$-1 \le f_i \le 1, \quad -1 \le g_i \le 1. \tag{14}$$

Thus, the second term on the right-hand side (RHS) of (13) is bounded by

$$-\sqrt{2} r_i \le r_i \cos(\theta_i) f_i + r_i \sin(\theta_i) g_i \le \sqrt{2} r_i. \tag{15}$$

The last term on the RHS of (13) is bounded by

$$\begin{aligned} -\alpha r_i(r_{i-1} + r_{i+1}) &\le \alpha(\bar{r}_i \cdot \bar{r}_{i-1} + \bar{r}_i \cdot \bar{r}_{i+1}) \\ &\le \alpha r_i(r_{i-1} + r_{i+1}). \end{aligned} \tag{16}$$

Using (15) and (16), an upper bound and a lower bound on (13) can be written as

$$\begin{aligned} -(1 + 2\alpha)r_i^2 - \sqrt{2} r_i - \alpha r_i(r_{i-1} + r_{i+1}) &\le r_i \dot{r}_i \\ &\le -(1 + 2\alpha)r_i^2 + \sqrt{2} r_i + \alpha r_i(r_{i-1} + r_{i+1}) \end{aligned} \tag{17}$$

which now places a finite bound on r_i as a function of α and n. If $\alpha = 0$, and we divide both sides by r_i, then (17) becomes

$$-r_i - \sqrt{2} \le \dot{r}_i \le -r_i + \sqrt{2} \tag{18}$$

which implies that $\dot{r} \leq 0$ if $r_i < \sqrt{2}$. Consequently, the bounds will reach an equilibrium such that $r_{\max}$, the maximum distance between any two connected oscillators, is less than, or equal to $\sqrt{2}$. Thus, without any coupling whatsoever, there is a finite bound on $r_{\max}$. Because the interaction terms are designed to give rise to synchrony, one would expect that they would have the effect of reducing $r_{\max}$. We now show that we can control the size of $r_{\max}$ by an appropriate choice of α. We divide (17) by r_i and examine only the upper bound, which we rewrite as matrix equation (19) shown at the bottom of the page, where $\boldsymbol{q} = (q_1, q_2, \cdots, q_{n-1})^t$ and $\boldsymbol{k}$ is a $(n-1)\times 1$ column vector of all "1's". Let $\boldsymbol{A}$ be the matrix in (19). We will use the convention of denoting vectors with lower case bold letters, and matrices with upper case bold letters. The superscript "t" denotes the transpose. The eigenvalues of $\boldsymbol{A}$ are all negative, thus (19) approaches an equilibrium value at an exponential rate. The equilibrium values of the elements in $\boldsymbol{q}$, which we denote with $\boldsymbol{q}^{eq}$, are defined by

$$\boldsymbol{q}^{eq} = -\frac{\sqrt{2}}{\alpha}\boldsymbol{A}^{-1}\boldsymbol{k}. \tag{20}$$

We multiply each side of (20) by $\boldsymbol{k}^t$ to obtain

$$\sum_{i=1}^{n-1} q_i^{eq} = -\frac{\sqrt{2}}{\alpha}\sum_{i,j=1}^{n-1}(A^{-1})_{ij}. \tag{21}$$

For $\alpha \gg 1$ we can approximate $\boldsymbol{A}$ with $\boldsymbol{B}$, where

$$\boldsymbol{B} = \begin{bmatrix} -2 & 1 & & & \\ 1 & -2 & 1 & & \\ & & \vdots & & \\ & & 1 & -2 & 1 \\ & & & 1 & -2 \end{bmatrix}. \tag{22}$$

The inverse of this matrix follows a regular pattern and we can explicitly write

$$-\sum_{i,j=1}^{n-1}(B^{-1})_{ij} = \tfrac{1}{2} + \tfrac{11}{12}(n-1) + \tfrac{1}{2}(n-1)^2 + \tfrac{1}{12}(n-1)^3. \tag{23}$$

Because the elements of $\boldsymbol{A}^{-1}$ change continuously and monotonically with α (see [8]), and also because $\boldsymbol{A}$ remains invertible in the range $0 < \alpha < \infty$, we can use (23) as an upper bound on the sum of all the elements in $\boldsymbol{A}^{-1}$, i.e.,

$$-\sum_{i,j=1}^{n-1}(A^{-1})_{ij} < -\sum_{i,j=1}^{n-1}(B^{-1})_{ij}. \tag{24}$$

We use (23) and (24) to bound (21) as

$$\sum_{i=1}^{n-1} q_i^{eq} < \frac{\sqrt{2}}{\alpha}\left[\frac{1}{2} + \frac{11}{12}(n-1) + \frac{1}{2}(n-1)^2 + \frac{1}{12}(n-1)^3\right]. \tag{25}$$

It can be shown that the elements of matrix $\boldsymbol{A}^{-1}$ are all negative. Given that the elements of $\boldsymbol{k}$ are all "1's", (20) implies that all the elements of $\boldsymbol{q}^{eq}$ are greater than zero. With this we can write the following inequality:

$$q_{\max}^{eq} \leq \sum_{i=1}^{n-1} q_i^{eq} \tag{26}$$

where $q_{\max}^{eq}$ is the maximum of the q_i^{eq}'s. (26) and (25) give the following inequality:

$$q_{\max}^{eq} < \frac{\sqrt{2}}{\alpha}\left[\frac{1}{2} + \frac{11}{12}(n-1) + \frac{1}{2}(n-1)^2 + \frac{1}{12}(n-1)^3\right]. \tag{27}$$

Assume that both systems of $\boldsymbol{r}$ and $\boldsymbol{q}$ start with the same initial conditions, i.e., $\boldsymbol{r}(0) = \boldsymbol{q}(0)$. Given that $\dot{\boldsymbol{r}} \leq \boldsymbol{A}\boldsymbol{r} + \sqrt{2}\boldsymbol{k}$ and $\dot{\boldsymbol{q}} = \boldsymbol{A}\boldsymbol{q} + \sqrt{2}\boldsymbol{k}$, it is known that $\boldsymbol{r}(t) \leq \boldsymbol{q}(t)$ for $t \geq 0$ [27]. Thus, after some time, (19) will reach equilibrium, and we can use (27) and that $r_{\max} \leq q_{\max}$ to write

$$r_{\max} < \frac{\sqrt{2}}{\alpha}\left[\frac{1}{2} + \frac{11}{12}(n-1) + \frac{1}{2}(n-1)^2 + \frac{1}{12}(n-1)^3\right] \tag{28}$$

(28) shows that for fixed n, $r_{\max}$ is bounded by a quantity that is inversely proportional to α. In essence, we can decrease $r_{\max}$ by increasing α. We use this control to further constrain the upper bound of (15), because once $r_{\max}$ is smaller than a certain value

$$r_f = \frac{2e}{(a^2+b^2)^{1/2}} \tag{29}$$

the maximal values for f_i and g_i are no longer equal to 1. According to (8) and (11), if $f_i = 1$ then one oscillator is at a location on the plane such that $ax_1 - by_1 - \varphi_x > e$, and the other oscillator must satisfy $ax_2 - by_2 - \varphi_x < -e$. In other words, the oscillators lie on opposite sides of the piece-wise linear function $P(v)$, and do not lie on the intermediate sloped line. r_f is the minimum distance between two oscillators such that $f_i = 1$. If the distance between two oscillators is less than r_f, then the two oscillators lie on the same, or adjacent, pieces of function $P(v)$ and thus $f_i < 1$. There is also a corresponding value r_g for the function g_i, but $r_f < r_g$ due to the constraint $a^2 + b^2 > c^2 + d^2$ previously mentioned. If $r_{\max} < r_f$ then

$$\dot{\boldsymbol{q}} = \alpha \begin{bmatrix} -1/\alpha - 2 & 1 & & & \\ 1 & -1/\alpha - 2 & 1 & & \\ & & \vdots & & \\ & & 1 & -1/\alpha - 2 & 1 \\ & & & 1 & -1/\alpha - 2 \end{bmatrix} \boldsymbol{q} + \sqrt{2}\boldsymbol{k} \tag{19}$$

automatically $r_{\max} < r_g$ which implies that $g_i < 1$. Thus we want to choose α such that

$$\alpha > \frac{(a^2+b^2)^{1/2}}{\sqrt{2}e}\left[\frac{1}{2}+\frac{11}{12}(n-1)+\frac{1}{2}(n-1)^2 + \frac{1}{12}(n-1)^3\right]. \tag{30}$$

If the inequality in (30) is satisfied, then $r_{\max}$ is less than r_f and, using (8) and (11), the functions f_i and g_i will have the following bounds:

$$\frac{-r_i}{2e}(a\cos(\theta_i) - b\sin(\theta_i)) \le f_i \le \frac{r_i}{2e}(a\cos(\theta_i) - b\sin(\theta_i)) \tag{31a}$$

$$\frac{-r_i}{2e}(c\cos(\theta_i) + d\sin(\theta_i)) \le g_i \le \frac{r_i}{2e}(c\cos(\theta_i) + d\sin(\theta_i)) \tag{31b}$$

which simplify to

$$\frac{-r_i}{2e}\sqrt{a^2+b^2} \le f_i \le \frac{r_i}{2e}\sqrt{a^2+b^2} \tag{32a}$$

$$\frac{-r_i}{2e}\sqrt{c^2+d^2} \le g_i \le \frac{r_i}{2e}\sqrt{c^2+d^2}. \tag{32b}$$

In (13) the terms involving f_i and g_i are multiplicative. Hence, $[r_i\cos(\theta_i)f_i + r_i\sin(\theta_i)g_i]$ is the function that must be examined. If $r_{\max} \le r_f$ we can use (32) to write

$$r_i\cos(\theta_i)f_i + r_i\sin(\theta_i)g_i \le \frac{r_i^2}{2e}\sqrt{a^2+b^2+c^2+d^2}. \tag{33}$$

For convenience, let

$$M = \frac{1}{2e}\sqrt{a^2+b^2+c^2+d^2}. \tag{34}$$

Using (34) and (16) an upper bound of (13) can be written as

$$r_i\dot{r}_i \le -(1+2\alpha)r_i^2 + Mr_i^2 + \alpha r_i(r_{i-1}+r_{i+1}) \tag{35}$$

which simplifies to

$$\dot{r}_i \le -(1+2\alpha)r_i + Mr_i + \alpha(r_{i-1}+r_{i+1}). \tag{36}$$

Letting $\beta = M - 1$ and

$$\boldsymbol{W} = \begin{bmatrix} \beta-2\alpha & \alpha & & & & & \\ \alpha & \beta-2\alpha & \alpha & & & & \\ & \alpha & \beta-2\alpha & \alpha & & & \\ & & & \vdots & & & \\ & & & \alpha & \beta-2\alpha & \alpha & \\ & & & & \alpha & \beta-2\alpha & \end{bmatrix} \tag{37}$$

we rewrite (36) as

$$\dot{\boldsymbol{r}} \le \boldsymbol{W}\boldsymbol{r} \tag{38}$$

Using the same logic which leads to (19), let

$$\dot{\boldsymbol{p}} = \boldsymbol{W}\boldsymbol{p}. \tag{39}$$

and assume that the initial conditions for both systems are identical, i.e., $\boldsymbol{p}(0) = \boldsymbol{r}(0)$, then $\boldsymbol{r}(t) \le \boldsymbol{p}(t)$ for $t > 0$. If all the eigenvalues of $\boldsymbol{W}$ are negative, then the matrix is stable. If the matrix is stable all the elements of $\boldsymbol{p}$ approach zero, which forces all the elements of $\boldsymbol{r}$ to approach zero. We now examine the eigenvalues of $\boldsymbol{W}$ to find under what conditions they become negative. The eigenvalues of $\boldsymbol{W}$ are given by

$$\lambda_k = (\beta - 2\alpha) - 2\alpha\cos\left(k\frac{\pi}{n}\right) \tag{40}$$

where $k = 1, 2, \cdots, n-1$ and $n \ge 3$. The condition for all eigenvalues to be negative can be written as

$$\alpha > \frac{\beta}{4\sin^2(\pi/2n)}. \tag{41}$$

For $n \gg 1$ this becomes

$$\alpha > \frac{\beta n^2}{\pi^2}. \tag{42}$$

In summary, synchrony will be asymptotically stable for the chain of coupled oscillators defined in (7) if α is chosen such that the inequalities in (30) and (41) are satisfied. This concludes the proof.

The reported time for a human subject to identify a single object is estimated to be less than 100 ms. [9]. If oscillatory correlation is used by the brain, synchrony must be achieved before identification takes place. Experimental evidence from the cat visual cortex shows that synchrony is achieved quickly, within 25–50 ms., or 1–2 cycles in 40 Hz oscillations [30]. These experimental results emphasize the importance of fast synchrony. From practical considerations synchrony must also be achieved quickly to deal with a rapidly changing environment. In this model we can control the rate of synchrony by increasing the coupling strength. But that would lead to unreasonably large values for α. This problem can be avoided by careful adjustment of the nullclines, and we now describe a method by which a chain of several hundred WC oscillators, as defined in (1), but arranged as a one dimensional chain, can be entrained within the first cycle.

Note that the method of entrainment described below takes place after the dynamic weights have attained their proper values. We neglect the initial transient dynamics of the network because they do not affect the properties of the system after an initial period. Our method of fast synchrony requires that there exist one region in the phase plane where the x and y nullclines of the oscillator are very near to one another. More specifically, in the system of (1), the parameters were chosen so that this occurs in the upper left-hand corner, as seen in Fig. 3. The oscillators travel slowly through this region because, close to the nullclines, the values of $\dot{x}$ and $\dot{y}$ are near zero. Note that this need not be true in general, but it is true in the smoothly varying WC equations that we use. The x and y nullclines are so near each other that only a small perturbation is needed to push the y nullcline to the left, and cause it to intersect the x nullcline (we will use the coupling term to create this perturbation). When the nullclines intersect, two new fixed points are created. One of these fixed points is attracting, and will stop periodic motion. We neglect the case when the nullclines just touch, as the single bifurcation point exists only momentarily, and does not significantly affect the dynamics.

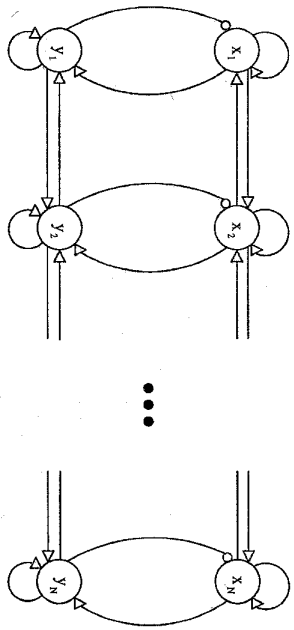

Fig. 5. A diagram showing the interactions between the excitatory and inhibitory units in a chain of oscillators. See the caption of Fig. 2 for the meaning of the notations.

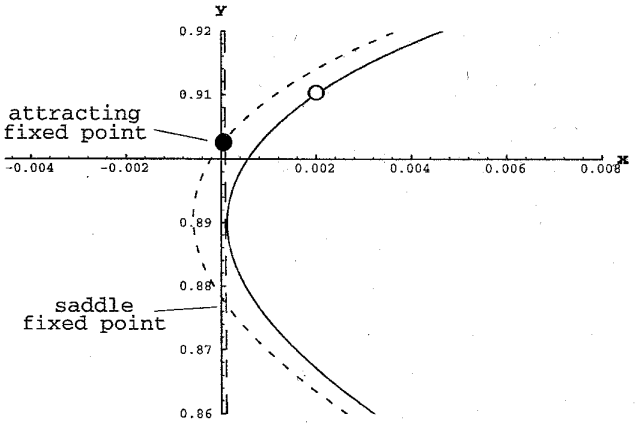

Fig. 6. An enlarged diagram of the upper left-hand corner of Fig. 3 that displays the nullclines of two interacting oscillators. The two dashed curves are the nullclines for the leading oscillator, and the black filled circle represents the position of the leading oscillator. The interaction term causes the y nullcline (short dashed curve) of the leading oscillator to be perturbed to the left so that it intersects the x nullcline (long dashed curve). This creates an attracting fixed point and a saddle fixed point. The interaction term does not impede the motion of the trailing oscillator (open circle), which will approximately follow the path given by the solid curve. The leading oscillator will be trapped at the attracting fixed point until the distance between the oscillators is very small.

Let us examine the case of two coupled oscillators in detail. Specifically, we examine two oscillators that are near to one another and approaching the upper left-hand corner of the unit square from the right, i.e., rotating counterclockwise. Fig. 6 displays an enlarged picture of this region. The interaction term will cause the x and y nullclines of the leading oscillator to intersect, effectively trapping it at the newly created fixed point. In Fig. 6 the leading oscillator (black filled circle) is shown trapped at the attracting fixed point, which is the top intersection of the x nullcline and the y nullcline. The other oscillator is represented by an unfilled circle, and its movement along the limit cycle is not impeded. As the oscillators come closer the interaction term decreases, and the y nullcline of the leading oscillator moves to the right. When the oscillators are close enough, the x and y nullclines of the leading oscillator will separate, releasing the leading oscillator from the fixed point and allowing its motion along the limit cycle to continue. We have ignored the motion of the x nullcline because it moves up and down only a small amount during this process. Since the x nullcline is almost completely vertical in this region, moving it by a small amount has a negligible effect. In summary, our method of fast synchrony requires that there be a region where the nullclines are very near to one another, and that the interaction terms be organized to alter the behavior of an oscillator in this region appropriately as described above.

The distance between the oscillators can be controlled precisely in this manner. It depends solely on the original separation of nullclines, and the size of α. To be more precise, for the parameters specified in the caption of Fig. 3, a y interaction term greater than 0.0003 will cause the nullclines to intersect. Thus, the distance between the oscillators in the y direction, $(y_2 - y_1)$, will have to be less than $(0.0003/\alpha)$ before periodic motion resumes. Because the oscillators are almost directly above one another, $x_2 \approx x_1$, and the distance between the oscillators can be approximated by $(0.0003/\alpha)$. This distance is orders of magnitude smaller than the size of the limit cycle, so we can safely call the oscillators separated by this distance synchronized. This phase adjustment, however, only occurs in the upper left-hand corner of the limit cycle. One must ensure that both oscillators are in this region and not on opposite sides of the limit cycle. We increase the value of α to make sure the oscillators approach each other before moving to the limit cycle. This behavior can be explained by examining only the interaction terms in (1) and ignoring the oscillatory terms. We find that the scalar diffusive coupling terms converge asymptotically to a single stable point. Thus, if α is sufficiently large, the interaction terms will dominate over the oscillatory terms, and cause the oscillators approach each other. As the oscillators come together, the interaction terms decrease, and the oscillatory terms start to contribute to the dynamics. So, with a sufficiently large α, the oscillators will be loosely synchronized before oscillatory motion starts. The oscillators will then approach the upper left-hand corner of the limit cycle. If the distance between the two oscillators is larger than $(0.0003/\alpha)$, then the interaction term will cause the nullclines of the leading oscillator to intersect. An attracting point will be created and the leading oscillator will be trapped at this point until the second oscillator moves to within a distance of $(0.0003/\alpha)$. In summary, α is used to loosely group the oscillators together. The oscillators then travel along the limit cycle to the upper left-hand corner, where they become tightly synchronized.

By controlling α and the position of the nullclines, we can reduce the distance between the two oscillators to an arbitrarily small value. Using these same techniques, we can control the overall entrainment of a chain of oscillators. Fig. 7 shows the x activities of 34 oscillators plotted on the same

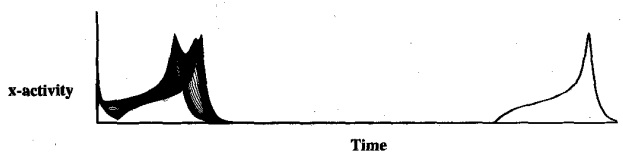

Fig. 7. This graph displays the combined x values of 34 oscillators with respect to time. An accurate synchrony is achieved within the first cycle. The random initial conditions used were restricted to the range of the limit cycle, i.e., $0.0 \leq x \leq 0.5$ and $0.0 \leq y \leq 1.0$. Parameters $\alpha = 14$ and $\sigma = 0$.

graph. The oscillators are those defined in (1), but they are arranged in a chain, and are not connected to GS. The strong interaction terms cause the oscillators to approach each other rapidly, creating a thick conglomeration of curves, instead of 34 completely random curves. These loosely synchronized oscillators will then approach the upper left-hand corner of the limit cycle, where they become tightly synchronized. By the next peak, one can see that only a single thin curve is exhibited, as all the oscillators are at virtually the same x value at the same time. We make no claims that an infinite number of oscillators can be entrained using this method. Large chain lengths (n > 500) could require excessively large coupling strengths. We are interested in finite systems and have tested this method with chain lengths up to several hundred oscillators. We conjecture that the behavior for a matrix of 256 × 256 locally coupled oscillators would be similar in terms of their synchronization.

The method described above can group many oscillators to within a small distance of one another, and therefore within a small distance of the in-phase solution. Because we have not shown that the actual WC oscillators synchronize, a variational analysis [45] is appropriate. In this analysis all the variables are perturbed by a small amount from a known solution, in this case, the synchronous solution. The perturbations are assumed to be sufficiently small so that their first-order approximations are valid. The properties of the resulting system of linear equations can then be examined. We assume the existence of a smooth stable limit cycle, and do not consider the effects of noise or GS. Our analysis has shown that the in-phase solution is locally stable. We omit the details of this straightforward procedure of the analysis.

Our model, as it stands, is not consistent with Dale's law, which states that neurons have only a single type of connection, either inhibitory or excitatory, to other neurons. As seen in Fig. 5, the y variables, which represent inhibitory populations of neurons, have both excitatory and inhibitory connections to other variables. Our model, however, can be readily made to conform to Dale's law by introducing inhibitory interneurons. For example, inhibitory interneurons can be introduced in place of excitatory connections between neighboring y units, so that the connections from units are inhibitory. We have not incorporated these interneurons because they would add complexity to the model without changing its overall behavior.

In summary, we have shown that the piece-wise linear form of the WC oscillator will synchronize if the coupling strength meets a certain criteria, and we have presented a method for rapid synchrony. In our simulations, we have used both the piece-wise linear approximation of the oscillator (7) and the actual WC oscillators (1), and observed that any positive coupling strength will give rise to synchrony, even if it does not satisfy the conditions previously specified. Therefore we conclude that synchrony can be achieved in populations of WC oscillators with local connections.

IV. Desynchronization

As discussed previously, a method of desynchronization is necessary for minimizing the possibility of accidental synchrony. Several models [53], [63] have methods of desynchronization, but it is not clear how these models perform with more than two objects. In Hansel and Sompolinsky [33], noise in a chaotic system is used to desynchronize objects, but noise can also lead to synchronizing objects. Hence this is not a reliable method of distinguishing multiple objects.

To reliably desynchronize multiple objects, independent oscillations in an oscillator network cannot be permitted. Thus we globally connect GS to and from every oscillator in the network so that no two oscillators act fully independently. These long-range connections serve to adjust phase relationships between oscillator groups representing different objects. GS has a minimum value of zero and is defined as

$$\dot{z} = \delta(1 - z)Tr - \nu z \tag{43}$$

Tr is a binary value, which is turned on (set to one) if any oscillator lies within a small region near the origin; it is defined as

$$Tr = \begin{cases} 1 & \text{if } (x_i + y_i) > \mu \\ 0 & \text{if otherwise} \end{cases} \qquad 1 \leq i \leq N. \tag{44}$$

The positive parameters δ and ν control the rate of growth and decay of z. We call this area near the origin the triggering region because when an oscillator enters this region, $Tr = 1$, and the value of GS starts to increase. μ controls the size of the triggering region. As seen in (1), the value of GS is fed into the x unit of every oscillator. This manipulation has the simple effect of raising or lowering the x nullcline of every oscillator. Fig. 8 displays the triggering region and its position relative to the nullclines. Just to the right of the triggering region there is another slow region, because the x and y nullclines are relatively close. All oscillators rotate counterclockwise, so an oscillator will enter the triggering region, and then pass through the slow region between the nullclines.

GS can only take on positive values, enabling it to raise nullclines or return them to their original positions. An oscillator in the triggering region will cause the x nullcline of every oscillator to rise, and will produce a marked increase the speed of those oscillators in the slow area. Because the triggering region and the slow region are adjacent, any two oscillators with nearby phases will be separated when the trailing oscillator enters the triggering region. The movement of the x nullclines will affect oscillators elsewhere on the limit cycle, but the change in their speed of motion will be negligible compared to the increase in speed received by an oscillator in the slow area.

Fig. 9 displays the ability of GS to separate two oscillators. The first two plots display the x activity of two oscillators

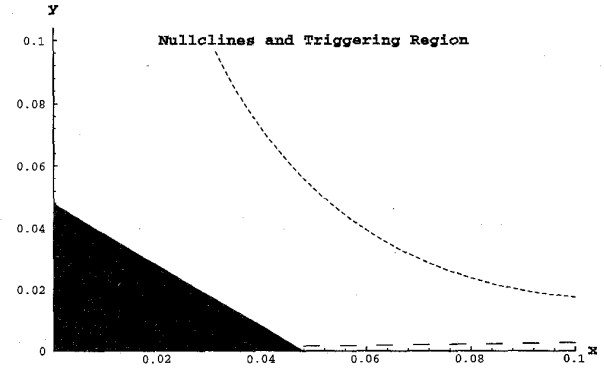

Fig. 8. A close look of the triggering region (black filled triangle), the x nullcline (short dashed curve), and the y nullcline (long dashed curve). The value $\mu = 0.048$ was used in the simulations, but other nearby values result in desynchronization also. The other parameters were $\delta = 2.9$ and $\nu = 2.0$.

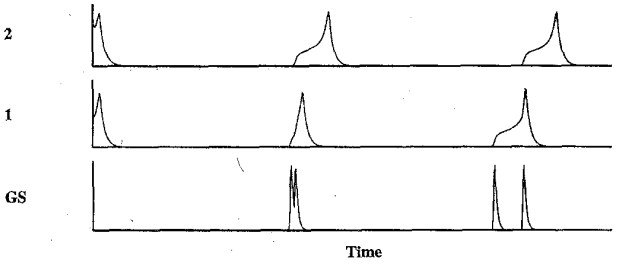

Fig. 9. The activities of two oscillators and the global separator are plotted with respect to time. The two oscillators are desynchronized during the second cycle. The shape of the first oscillator is significantly altered because its speed is increased by GS. All parameters are the same as those previously listed in Figs. 3 and 8.

in time. The third plot is the activity of GS with respect to time. The oscillators are almost in phase in the first cycle, but a major shift occurs during the second cycle. This occurs when oscillator 2, which trails oscillator 1, enters the triggering region and thus excites GS, which then increases the speed of oscillator 1. The sharp change in the characteristic shape of oscillator 1 during the second cycle demonstrates the increase in speed induced by GS while oscillator 1 was within the slow region. Afterward, GS continues to cause minor phase shifts during every cycle. These small phase shifts slowly decrease as the relative phase difference increases. Eventually, an equilibrium is attained. The equilibrium, however, does not ensure an antiphase relationship between the two oscillators, but suffices to clearly distinguish their phases.

Naturally, the desynchronization of objects by this method acts in direct opposition to the necessity of achieving synchrony within groups of oscillators. We resolve this problem by increasing the coupling strength. Increased coupling maintains synchrony within groups of connected oscillators, but does not alter the performance of GS because it does not change the shape of the limit cycle.

V. Simulation Results

We now discuss the simulation results of this model using the input displayed in Fig. 4. Fig. 10(a)–(f) displays network activity at specific time steps during numerical integration.

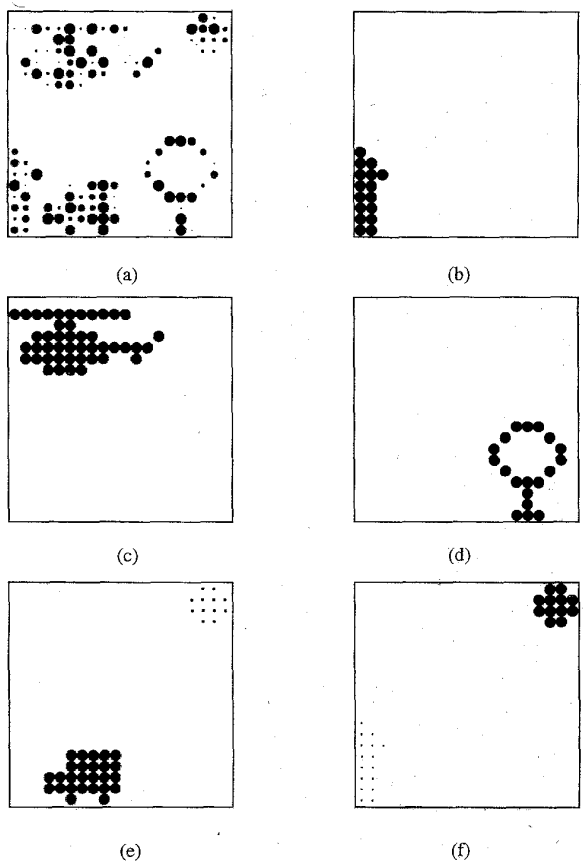

Fig. 10. Each picture represents network activity at a time step in the numerical simulation. The size of the circle is proportional to the x activity of the corresponding oscillator. (a) The oscillators have random positions on the phase plane at the first time step. (b)–(f) Successive time steps that correspond to the maximal activities for each group of oscillators. $\alpha = 10.0$ in this simulation. The other parameters are as specified in the captions of Figs. 3 and 8. The random initial conditions used were restricted to the range of the limit cycle, namely, $0.0 \leq x \leq 0.5$ and $0.0 \leq y \leq 1.0$.

Fig 10(a) represents the initial activity of the network. The sizes of the circles are directly proportional to the x values of the corresponding oscillators. The random sizes of the circles in Fig. 10(a) represent the random initial conditions of the oscillators. Fig. 10(b) is a later time step when the object that resembles a house is at its highest activation. Fig. 10(c) displays the time step after Fig. 10(b) when the object resembling a helicopter is maximally active. Fig. 10(d) corresponds to the time step after Fig. 10(c) when the highest activation for the tree-like object is attained. This object was specifically selected to emphasize that any connected region will synchronize, whether it is concave or convex. Fig. 10(e) shows a later time step when the truck shaped object is maximally activated. The object resembling a thick addition symbol is also weakly activated at this time step. Finally, Fig. 10(f) shows the time step when the thick addition sign is at its highest activation. The objects clearly "pop out" once every cycle.

In Fig. 11, we display the activities of GS and the x activities of all stimulated oscillators for the first few cycles. The first five plots display the combined x activities of all

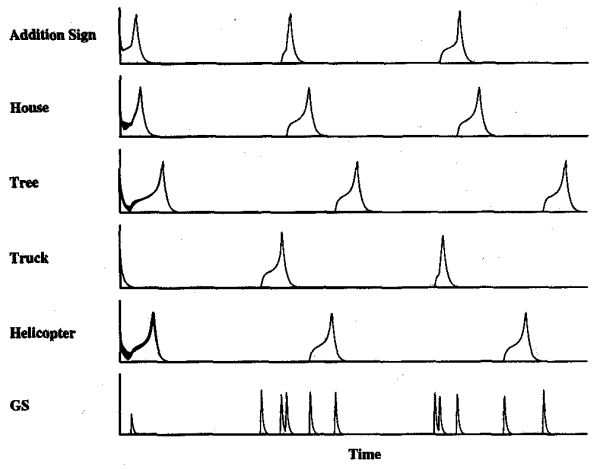

Fig. 11. The plot labeled "GS" displays the activity of the global separator with respect to time. The other five plots display the combined x activities of all the oscillators stimulated by the corresponding object. Each of the five oscillator groups is synchronized within the first cycle, and by the second cycle is desynchronized from the other oscillator groups.

oscillators that are stimulated by the five objects. Each of the properties we have described in previous sections are shown in this graph. Initially the interaction terms dominate and cause the oscillators to loosely synchronize. Loose synchrony is seen on the graph by observing that each of plots quickly merge into a thick line. By the second peak, the oscillators have been synchronized to such a degree that only a thin single curve is exhibited. Desynchronization most noticeably occurs during the fourth activation of GS. The phase difference between the oscillator groups representing the house and the addition sign is significantly altered at this time. This shift in phase is signaled by the change in the characteristic shape of the oscillator group representing the addition sign. The activity of GS is displayed on the last frame of Fig. 11. GS is activated when any oscillator, or oscillator group passes through the triggering region. When the oscillators are well separated, GS will be active five times per cycle, signaling successive "pop outs" of the five objects. Only the first three cycles are depicted in this graph, but as we have tested, synchrony within the oscillator groups, as well as desynchrony between the groups is maintained afterwards without degradation.

We can reliably separate up to at least nine objects (results not shown). Separating the phases of more objects becomes increasingly difficult for this system. The finite time required for an oscillator to travel through the triggering region, and the finite area affected by GS, constrain the number of objects that can be separated. This limitation seems consistent with the well-known psychological result that humans have a fundamental bound on the number of objects that can be held in their attentional span [43].

Even though noise was not used in the simulations presented here, we have tested the network with various amounts of noise. As expected, the system is robust for small amounts of noise, but cannot tolerate very large quantities. This is because noise by itself can cause the nullclines to intersect and thus interfere with the mechanism we use to synchronize oscillators. The amount of noise the system can tolerate increases with the size of the coupling strength.

We used the numerical ordinary differential equation (ODE) solvers found in [49] to conduct the above simulations. An adaptive Runga–Kutta method was used for most of the simulations reported. The Bulrisch–Stoer method was later used to confirm the numerical results. The network had the same dynamics with either of the integration methods. So it is very unlikely that numerical errors played any significant role in our simulation results.

VI. Discussion

Our analysis of the WC oscillator network demonstrates that it contains the basic features necessary to achieve oscillatory correlation. This includes: dynamic couplings, short-range excitatory connections to synchronize oscillators, and long-range excitatory connections to desynchronize groups of oscillators. With this simple architecture, we have used the theory of oscillatory correlation, together with the Gestalt principle of connectedness to illustrate sensory segmentation. The model retains information of spatial relationships through local coupling, and does not suffer from the problems of accidental synchrony through the use of a global separator to segregate objects.

Although we have not attempted to simulate the experimental findings of Gray *et al.* [31], the network is neurally plausible. The WC equations represent the activities of neural groups, and local excitatory connections are consistent with lateral connections widely seen in the brain [38]. The global separator may be viewed as part of an attentional mechanism. Experiments conducted by Treisman and Gelade [61] suggest that if an object has several features, a correct conjunction of those features relies on attention. Thus, if feature binding is achieved through oscillatory correlation, the attentive mechanism may serve to synchronize features into a coherent object, as well as segment different objects. In performing desynchronization, GS may accomplish a task that is fundamental to attention. GS also has structural similarities to a proposed neural attentional mechanism. Crick [15] suggested that the reticular complex of the thalamus may control attention, in part because it has connections both to and from many regions of the cortex. Thus, the reticular complex of the thalamus may have influence over widely separated sensory processing regions. With its wide range couplings, GS may have structural, as well as functional, relations to the proposed attentional mechanisms.

We have shown that synchrony can occur in locally coupled oscillators if the coupling is sufficiently large. This is proven using the piece-wise linear approximation to the WC oscillators. Numerically we observe that synchrony occurs, with local coupling, in the actual WC oscillators (1), as well as our approximation to them (7), with any positive coupling strength. This implies that synchrony in such oscillator networks is possible with local connections only. We have also demonstrated a method that can synchronize large numbers of oscillators within the first cycle. The method is based only on the position of the nullclines, and a property of the coupling. This technique is not specific to WC oscillators, or even scalar diffusive

coupling. It should be applicable to other types of oscillators as well. We also present a mechanism for desynchronization, which can segment up to nine spatially separate objects. Our mechanism requires only a basic control of speed through a single region of the limit cycle, so it too can be transferred to other oscillator models (see also [60] and [69]).

Our method of fast synchronization requires a region in which two nullclines are very near to each other. Because of this, noise that alters the position of these nullclines with respect to one another may destroy fast synchrony, or stop the periodic motion of some oscillators completely. The former case can occur with the form of noise defined in (2), which is added into the sigmoid term as in (1). The latter case can occur when the dynamic coupling is imperfect, e.g., if a constant noise term is added to (5). A robust system should exhibit properties of synchrony and desynchrony in the presence of noisy input, with oscillators that contain internal noise, and also with connections that can introduce some form of noise. In this respect, out study suggests that the WC oscillators with scalar diffusive coupling may not be able to support as robust synchronization and desynchronization as the relaxation oscillators networks studied in [60] and [69].

The matrix analysis we have done for a chain of oscillators can be extended to analyze higher-dimensional oscillator lattices. We conjecture that synchrony can also be achieved in more than two dimensions, with only a positive coupling strength. This is based on simulations that we have done with 2-D grids that exhibit the same phase locking behavior as we have seen in one-dimensional chains. Also, this analysis can be done with lateral connections farther than nearest-neighbor connections. In fact, numerical simulations (data not shown) in one and two dimensions show that longer range connections can even facilitate synchronization. We speculate that analysis with longer-range connections would indicate a decrease in the connection strength required to achieve synchrony.

Aside from explaining what may occur in the brain, oscillatory correlation offers a unique approach to the engineering of pattern segmentation, figure/ground segregation, and feature binding. Due to the nature of the oscillations, only a single object is active at any given time, and multiple objects are sequentially activated. The model can be used as a framework upon which more sophisticated methods of segmentation can be built. For example, the network can be extended to handle gray level input also. Dynamic couplings between excited neighboring oscillators could then be based on the contrast in the gray level of the stimulus. Regions with smoothly changing input would be grouped together, and segmented from regions with boundaries of sharp changes in gray level.

A unique advantage of using oscillatory correlation for perceptual organization is that the architecture is inherently parallel. Each oscillator operates simultaneously with all the others, and computations are based only on connections and oscillations, both of which are particularly feasible for VLSI (very large scale integration) chip implementation (for an actual chip implementation exploring phase locking see [3]). It also provides an elegant representation for real time processing. Given the enormous amount of information processing required by sensory processing, a parallel architecture and the potential for VLSI implementation are both very desirable qualities.

Perceptual tasks involving neural oscillations have also been observed in audition [26], [42], (see [67] for a model), and olfaction [25]. Oscillations have also been explored in associative recall networks [11], [68], [1]. With its computational properties plus the support of biological evidence, this model may offer a general approach to pattern segmentation and figure/ground segregation.

ACKNOWLEDGMENT

The authors would like to thank Profs. C. Jayaprakash and D. Terman for stimulating discussions.

REFERENCES

[1] L. F. Abbott, "A network of oscillators," *J. Phys. A*, vol. 23, pp. 3835–3859, 1990.
[2] M. Abeles, *Local Cortical Circuits*. New York: Springer-Verlag, 1982.
[3] A. G. Andreou and T. G. Edwards, "VLSI phase locking architectures for feature linking in multiple target tracking systems," in *Advances in Neural information Processing Systems 6*, J. D. Cowan, G. Tesauro, and J. Alspector, Eds. San Mateo, CA: Morgan Kaufmann, 1994.
[4] D. G. Aronson, G. B. Ermentrout, and N. Kopell, "Amplitude response of coupled oscillators," *Physica D*, vol. 41, pp. 403–449, 1990.
[5] B. Baird, "Nonlinear dynamics of pattern formation and pattern recognition in the rabbit olfactory bulb," *Physica D*, vol. 22, pp. 150–175, 1986.
[6] P. Baldi and R. Meir, "Computing with arrays of coupled oscillators: An application to preattentive texture discrimination," *Neural Computa.*, vol. 2, pp. 458–471, 1990.
[7] K. Bar-Eli, "On the stability of coupled chemical oscillators," *Physica D*, vol. 14, pp. 242–252, 1985.
[8] R. Bellman, *Introduction to Matrix Analysis*, 2nd ed. New York: McGraw-Hill, 1970.
[9] I. Biederman, "Recognition-by-components: A theory of human image understanding," *Psych. Rev.*, vol. 94, pp. 115–147, 1987.
[10] G. N. Borisyuk, R. M. Borisyuk, and A. I. Khibnik, "Bifurcation analysis of a coupled neural oscillator system with application to visual cortex modeling," in *Neural Information Processing Systems—Natural and Synthetic*, S. J. Hanson, J. D. Cowan, and L. Giles, Eds. San Mateo, CA: Morgan Kaufmann, 1993.
[11] J. Buhmann, "Oscillations and low firing rates in associative memory neural networks," *Phys. Rev. A*, vol. 40, pp. 4145–4148, 1989.
[12] D. E. Cairns, R. J. Baddeley, and L. S. Smith, "Constraints on synchronizing oscillator networks," *Neural Computa.*, vol. 5, pp. 260–266, 1993.
[13] T. Chawanya, T. Aoyagi, I. Nishikawa, K. Okuda, and Y. Kuramoto, "A model for feature linking via collective oscillations in the primary visual cortex," *Biol. Cybern.*, vol. 68, pp. 483–490, 1993.
[14] A. H. Cohen, P. J. Holmes, and R. H. Rand, "The nature of coupling between segmental oscillators of the Lamprey spinal generator for locomotion: A mathematical model," *J. Math. Biol.*, vol. 13, pp. 345–369, 1982.
[15] F. Crick, "Function of the thalamic reticular complex: The searchlight hypothesis," in *Proc. Nat. Acad. Sci. USA*, vol. 81, 1984, pp. 4586–4590.
[16] H. Daido, "Lower critical dimension for populations of oscillators with randomly distributed frequencies: A renormalization-group analysis," *Phys. Rev. Lett.*, vol. 61, pp. 231–234, 1988.
[17] R. Eckhorn, R. Bauer, W. Jordan, M. Brosch, W. Kruse, M. Munk, and H. J. Reitboeck, "Coherent oscillations: A mechanism of feature linking in the visual cortex?" *Biol. Cybern.*, vol. 60, pp. 121–130, 1988.
[18] G. M. Edelman, *Neural Darwinism: The Theory of Neuronal Group Selection*. New York: Basic Books, 1987.
[19] A. K. Engel, P. König, A. K. Kreiter, and W. Singer, "Synchronization of oscillatory neuronal responses between striate and exstriate visual cortical areas of the cat," in *Proc. Nat. Acad. Sci. USA*, vol. 88, 1991, pp. 6048–6052.
[20] ——, "Interhemispheric synchronization of oscillatory neuronal responses in cat visual cortex," *Sci.*, vol. 252, pp. 1177–1179, 1991.
[21] G. B. Ermentrout, "Oscillator death in populations of 'all to all coupled' nonlinear oscillators," *Physica D*, vol. 41, pp. 219–231, 1990.

[22] G. B. Ermentrout and J. D. Cowan, "Temporal oscillations in neuronal nets," *J. Math. Biol.*, vol. 7, pp. 265–280, 1979.
[23] G. B. Ermentrout and N. Kopell, "Oscillator death systems of coupled neural oscillators," *SIAM J. Appl. Math.*, vol. 50, pp. 125–146, 1990.
[24] J. L. Feldman and J. D. Cowan, "Large scale activity in neural nets II: A model for the brainstem respiratory oscillator," *Biol. Cybern.*, vol. 17, pp. 39–51, 1975.
[25] W. J. Freeman, "Spatial properties of an EEG event in the olfactory bulb and cortex," *Electroencephalogr. Clin. Neurophysiol.*, vol. 44, pp. 586–605, 1978.
[26] R. Galambos, S. Makeig, and P. J. Talmachoff, "A 40-Hz auditory potential recorded from the human scalp," in *Proc. Nat. Acad. Sci. USA*, vol. 78, 1981, pp. 2643–2647.
[27] M. Golomb and M. Shanks, *Elements of Ordinary Differential Equations*, 2nd ed. New York: McGraw-Hill, 1965.
[28] E. R. Grannan, D. Kleinfeld, and H. Sompolinsky, "Stimulus-dependent synchronization of neuronal assemblies," *Neural Computa.*, vol. 5, pp. 550–569, 1993.
[29] M. Grattarola and V. Torre, "Necessary and sufficient conditions for synchronization of nonlinear oscillators with a given class of coupling," *IEEE Trans. Circuits Syst.*, vol. 22, pp. 209–215, 1977.
[30] C. M. Gray, A. K. Engel, P. König, and W. Singer, "Temporal properties of synchronous oscillatory neuronal interactions in cat striate cortex," in *Nonlinear Dynamics and Neural Networks*, H. G. Schuster and W. Singer, Eds. Weinheim, Germany: VC Henry Verlangsgesellschaft, 1991.
[31] C. M. Gray, P. König, A. K. Engel, and W. Singer, "Oscillatory responses in cat visual cortex exhibit inter-columnar synchronization which reflects global stimulus properties," *Nature*, vol. 338, pp. 334–337, 1989.
[32] S. Grossberg and D. Somers, "Synchronized oscillations during cooperative feature linking in a cortical model of visual perception," *Neural Networks*, vol. 4, pp. 453–466, 1991.
[33] D. Hansel and H. Sompolinsky, "Synchronization and computation in a chaotic neural network," *Phys. Rev. Let.*, vol. 68, pp. 718–721, 1992.
[34] R. M. Haralick and L. G. Shapiro, "Image segmentation techniques," *Comput. Graphics Image Processing*, vol. 29, pp. 100–132, 1985.
[35] D. Horn, D. Sagi, and M. Usher, "Segmentation, binding and illusory conjunctions," *Neural Computa.*, vol. 3, pp. 510–525, 1991.
[36] J. E. Hummel and I. Biederman, "Dynamic binding in a neural network for shape recognition," *Psych. Rev.*, vol. 99, pp. 480–517, 1992.
[37] D. M. Kammen, P. J. Holmes, and C. Koch, "Cortical architecture and oscillations in neuronal networks: Feedback versus local coupling," in *Models of Brain Functions*, R. M. J. Cotterill, Ed. Cambridge, England: Cambridge Univ. Press, 1989, pp. 273–284.
[38] E. R. Kandel, J. H. Schwartz, and T. M. Jessell, *Principles of Neural Science*, 3rd ed. New York: Elsevier, 1991.
[39] T. Kawahara, K. Katayama, and T. Nogawa, "Nonlinear equations of reaction-diffusion type for neural populations," *Biol. Cybern.*, vol. 48, pp. 19–25, 1983.
[40] P. König and T. Schillen, "Stimulus-dependent assembly formation of oscillatory responses: I. Synchronization, *Neural Computa.*, vol. 3, pp. 155–166, 1991.
[41] Y. Kuramoto and I. Nishikawa, "Statistical macrodynamics of large dynamical systems—Case of a phase transition on oscillator communities," *J. Statist. Phys.*, vol. 49, pp. 569–605, 1987.
[42] C. Madler and C. Poppel, "Auditory evoked potentials indicate the loss of neuronal oscillations during general anesthesia," *Naturwissenschaften*, vol. 74, pp. 42–43, 1987.
[43] G. A. Miller, "The magical number seven, plus or minus two: Some limits on our capacity for processing information," *Psych. Rev.*, vol. 63, pp. 81–97, 1956.
[44] P. M. Milner, "A model for visual shape recognition," *Psych. Rev.*, vol. 81, pp. 521–535, 1974.
[45] N. Minorsky, *Nonlinear Oscillations*. Princeton, N.J.: Van Nostrand, 1962, pp. 124–133.
[46] T. Murata and H. Shimizu, "Oscillatory binocular systems and temporal segmentation of stereoscopic depth surfaces," *Biol. Cybern.*, vol. 68, pp. 381–391, 1993.
[47] V. N. Murthy and E. E. Fetz, "Coherent 25- to 35-Hz oscillations in the sensorimotor cortex of awake behaving monkeys," in *Proc. Nat. Acad. Sci. USA*, vol. 89, 1992, pp. 5670–5674.
[48] J. C. Neu, "Large populations of coupled chemical oscillators," *SIAM J. Appl. Math.*, vol. 38, pp. 305–316, 1980.
[49] W. H. Press, S. A. Teukolsky, W. T. Vetterling, and B. P. Flannery, *Numerical Recipes in C: The Art of Scientific Computing*, 2nd ed. Cambridge, England: Cambridge Univ. Press, 1992, pp. 710–734.
[50] I. Rock and S. Palmer, "The legacy of Gestalt psychology," *Sci. Amer.*, vol. 263, pp. 84–90, 1990.
[51] J. N. Sanes and J. P. Donoghue, "Oscillations in local field potentials of the primate motor cortex during voluntary movement," in *Proc. Nat. Acad. Sci. USA*, vol. 90, 1993, pp. 4470–4474.
[52] S. Sarkar and K. L. Boyer, "Perceptual organization in computer vision: a review and a proposal for a classificatory structure," *IEEE Trans. Syst., Man, Cybern.*, vol. 23, pp. 382–399, 1993.
[53] T. B. Schillen and P. König, "Stimulus-dependent assembly formation of oscillatory responses—II: Desynchronization," *Neural Computa.*, vol. 3, pp. 155–166, 1991.
[54] I. Schreiber and M. Marek, "Strange attractors in coupled reaction-diffusion cells," *Physica D*, vol. 5, pp. 258–272, 1982.
[55] H. G. Schuster and P. Wagner, "A model for neuronal oscillations in the visual cortex," *Biol. Cybern.*, vol. 64, pp. 77–82, 1990.
[56] D. Somers and N. Kopell, "Rapid synchronization through fast threshold modulation," *Biol. Cybern.*, vol. 68, pp. 393–407, 1993.
[57] H. Sompolinsky, D. Golomb, and D. Kleinfeld, "Cooperative dynamics in visual processing," *Phys. Rev. A*, vol. 43, pp. 6990–7011, 1991.
[58] O. Sporns, J. A. Gally, G. N. Reeke Jr., and G. M. Edelman, "Reentrant signaling among simulated neuronal groups leads to coherency in their oscillatory activity," in *Proc. Nat. Acad. Sci. USA*, vol. 86, 1989, pp. 7265–7269.
[59] S. H. Strogatz and R. E. Mirollo, "Phase-locking and critical phenomena in lattices of coupled nonlinear oscillators with random intrinsic frequencies," *Physica D*, vol. 31, pp. 143–168, 1988.
[60] D. Terman and D. L. Wang, "Global competition and local cooperation in a network of neural oscillators," *Physica D*, vol. 81, pp. 148–176, 1995.
[61] A. M. Treisman and G. Gelade, "A feature-integration theory of attention," *Cog. Psych.*, vol. 12, pp. 97–136, 1980.
[62] C. von der Malsburg, "The correlation theory of brain functions," Max-Planck-Institute for Biophysical Chemistry, Göttingen, Germany, Internal Rep. 81-2, 1981.
[63] C. von der Malsburg and J. Buhmann, "Sensory segmentation with coupled neural oscillators," *Biol. Cybern.*, vol. 67, pp. 233–246, 1992.
[64] C. von der Malsburg and W. Schneider, "A neural cocktail-party processor," *Biol. Cybern.*, vol. 54, pp. 29–40, 1986.
[65] D. L. Wang, "Modelling global synchrony in the visual cortex by locally coupled neural oscillators," in *Proc. 15th Annu. Conf. Cognit. Sci. Soc.*, 1993, pp. 1058–1063.
[66] ——, "Emergent synchrony in locally coupled neural oscillators," *IEEE Trans. Neural Networks*, vol. 6, no. 4, pp. 941–948, July 1995.
[67] ——, "An oscillatory correlation theory of temporal pattern segmentation," in *Neural Representation of Temporal Patterns*, E. Covey, H. Hawkins, T. McMullen and R. Port, Eds. New York: Plenum, in press, 1996.
[68] D. L. Wang, J. Buhmann, and C. von der Malsburg, "Pattern segmentation in associative memory," *Neural Computa.*, vol. 2, pp. 94–106, 1990.
[69] D. L. Wang and D. Terman, "Locally excitatory globally inhibitory oscillator networks," *IEEE Trans. Neural Networks*, vol. 6, pp. 283–286, 1995.
[70] H. R. Wilson and J. D. Cowan, "Excitatory and inhibitory interactions in localized populations of model neurons," *Biophys. J.*, vol. 12, pp. 1–24, 1972.
[71] S. M. Zeki, "The visual image in mind and brain," *Sci. Amer.*, vol. 265, pp. 69–76, Sept. 1992.

Shannon Campbell was born in New Orleans, LA, in 1969. He received the B.S. degrees in physics and applied mathematics from the University of California at Davis in 1990. Currently, he is a Ph.D. candidate in the Department of Physics at Ohio Sate University, Columbus.

His research interests include nonlinear dynamical systems, neural networks, and visual and auditory processing.

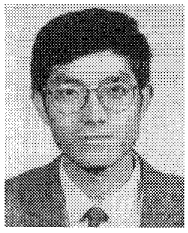

DeLiang Wang (M'94) was born in Anhui, the People's Republic of China in 1963. He received the B.Sc. degree in 1983 and the M.Sc. degree in 1986 from Beijing University, Beijing, China, and the Ph.D. degree in 1991 from the University of Southern California, Los Angeles, CA, all in computer science.

From July 1986 to December 1987 he was with the Institute of Computing Technology, Academia Sinica, Beijing. He is currently an Assistant Professor of Department of Computer and Information Science and Center for Cognitive Science at Ohio State University, Columbus, OH. His research interests include temporal pattern processing, auditory and visual pattern perception, neural network theories, and computational neuroscience.

Dr. Wang is a member of the IEEE Computer Society, the IEEE Systems, Man, and Cybernetics Society, the International Neural Network Society, and AAAS.